

# RSC Advances



This is an *Accepted Manuscript*, which has been through the Royal Society of Chemistry peer review process and has been accepted for publication.

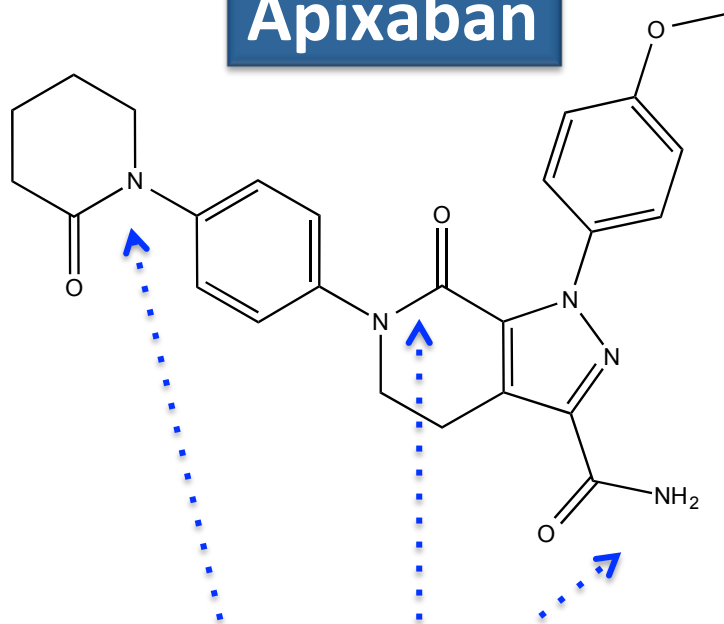
*Accepted Manuscripts* are published online shortly after acceptance, before technical editing, formatting and proof reading. Using this free service, authors can make their results available to the community, in citable form, before we publish the edited article. This *Accepted Manuscript* will be replaced by the edited, formatted and paginated article as soon as this is available.

You can find more information about *Accepted Manuscripts* in the [Information for Authors](#).

Please note that technical editing may introduce minor changes to the text and/or graphics, which may alter content. The journal's standard [Terms & Conditions](#) and the [Ethical guidelines](#) still apply. In no event shall the Royal Society of Chemistry be held responsible for any errors or omissions in this *Accepted Manuscript* or any consequences arising from the use of any information it contains.

# Degradation products

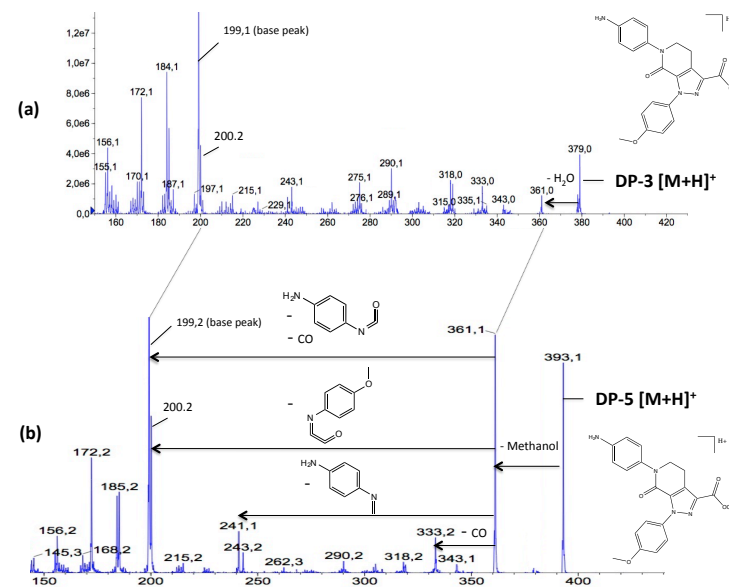
## Apixaban



Stress conditions

## Structural elucidation

LC-MS<sup>n</sup> and LC-HR-MS analysis





36 were generated for about 15 % of drug degradation. The degradation products have been  
37 detected by linear gradient reversed phase high-performance liquid chromatography coupled  
38 with photo diode array and with electrospray ionization tandem mass spectrometry.  
39 Combination of multistage mass spectrometry and of high-resolution mass spectrometry  
40 (HR-MS) allowed the structural elucidation. The product ions of the degradation products  
41 were compared to those of apixaban protonated ion so to assign the most structures  
42 possible. This had required a study in depth of the drug's fragmentation pattern, which has  
43 not been reported so far. In view of the products formed, it appears that hydrolysis of the  
44 oxopiperidin moiety of apixaban occurred in acidic medium, whereas that of the tetrahydro-  
45 oxo-pyridine moiety would further happen under alkali conditions. Besides from  
46 characterization, LC method was shown stability indicating and validated as per the criteria  
47 described by the ICH guidelines.

48

## 49 INTRODUCTION

50

51 Apixaban (1-(4-methoxyphenyl)-7-oxo-6-[4-(2-oxopiperidin-1-yl)phenyl]-4,5-  
52 dihydropyrazolo[5,4-c]pyridine-3-carboxamide) is a novel anticoagulant drug acting as direct,  
53 selective and reversible inhibitor of the coagulation factor Xa<sup>1-4</sup>. It is prescribed as treatment  
54 of venous thromboembolism, which includes deep vein thrombosis and pulmonary embolism.  
55 A large scale randomized double blind study comparing the conventional therapy  
56 (subcutaneous enoxaparin, followed by warfarin) to apixaban, showed the non-inferiority of  
57 apixaban with significant less bleeding<sup>5,6</sup>.

58 LC-MS/MS methods were developed to determine apixaban alone in plasma or in the  
59 presence of its major metabolites<sup>7-11</sup> to support clinical uses. Assay in tablets and  
60 simultaneous determination with other drugs using HPLC was also described<sup>12,13</sup>. A literature  
61 survey, however, did not reveal any further information about the stability profile of apixaban  
62 or about its potential degradation products likely to form in time and/or under stress

63 conditions. As drug may undergo degradations, leading potentially to activity loss or to  
64 occurrence of adverse effects associated with the appearance of degradation products,  
65 thorough knowledge of drug's stability profile is one of the key factors to prevent those risks  
66 during manufacturing, transportation and storage.

67 In this paper, we have focused on the identification and the characterization of degradation  
68 products generated in solution. Liquid chromatography combined with mass spectrometry  
69 has been well established and found to be a very useful technique for the identification and  
70 characterization of DPs<sup>14-17</sup>. That's why high performance liquid chromatography coupled with  
71 multistage mass spectrometry (HPLC-MS<sup>n</sup>) was used. Different stress conditions were  
72 applied in order to simulate the degradation of active pharmaceutical substances, for which  
73 degradation can occur via many pathways such as basic and acidic hydrolysis, oxidation,  
74 photo-degradation or thermal degradation. The structures of observed degradation products  
75 were elucidated using multistage mass spectrometry and high-resolution mass spectrometry  
76 (HR-MS). A study in depth of apixaban fragmentation pattern was also achieved in order to  
77 help assign, by comparison, the structures of the major product ions coming from the  
78 degradation products ions. In addition, LC-UV method for quantitative determinations of  
79 apixaban in the presence of its degradation products has been validated as per ICH<sup>18</sup>.

80

## 81 EXPERIMENTAL

82

### 83 Chemicals, reagents and stock standard solution

84

85 Apixaban (MW: 459. 4971g mol<sup>-1</sup>) tablets (Eliquis<sup>®</sup>) are marketed by Bristol-Myers Squibb  
86 (Rueil Malmaison, France) / Pfizer (Paris, France). A stock standard solution of apixaban was  
87 prepared by extracting apixaban from crushed tablets using water/methanol 50/50 to get a  
88 final concentration of 250 µg mL<sup>-1</sup>. Analytical grade acetonitrile came from Sigma-Aldrich (St

89 Quentin-Fallavier, France). Ultrapure water was produced by the Q-Pod Milli-Q system  
90 (Millipore, Molsheim, France). Hydrogen peroxide (H<sub>2</sub>O<sub>2</sub>) 30 % v/v was supplied by Carlo  
91 Erba SDS (Val de Reuil, France).

92

## 93 Instrumentation

94

95 LC-MS<sup>n</sup> analyses were performed using a Dionex Ultimate 3000 system (DIONEX, Ullis,  
96 France) coupled to a triple quadrupole linear ion trap HybridQtrap 3200 MS (ABSciex  
97 Framingham, USA) system. LC-HR-MS was performed coupling this same LC system to an  
98 LTQ-Orbitrap Velos Pro system, composed of a double linear trap and an orbital trap  
99 (Thermo Fisher Scientific, CA, USA). LC system consisted of a quaternary pump, a  
100 degasser, a thermostated autosampler with a 100 µL - injection syringe and a thermostated  
101 column compartment. Separation was achieved using Zorbax<sup>®</sup> column SB-C18 (4.6 mm x  
102 250 mm, i.d., 3.5 µm) kept at 25 °C in a thermostated compartment. The flow rate was set at  
103 1.0 mL min<sup>-1</sup>. A multi-stage gradient mobile phase (acetonitrile / water) was applied (Table  
104 1).

105

106 **Table 1.** HPLC gradient program.

107

108 Detection and characterization were performed by mass spectrometry and high-resolution  
109 mass spectrometry. In both cases, an electro-spray ionisation (ESI) source operated in  
110 positive ion mode. In MS, the ionization conditions were set as following: ion spray-voltage  
111 was set at 5.5 kV, curtain gas (N<sub>2</sub>) flow rate at 40 psi, nebulizer gas (air) flow rate at 30 psi  
112 and heater gas (air) flow rate at 50 psi. Temperature was set at 500 °C. Nitrogen was used  
113 as collision and damping gas. Acquisition in full scan mode over the mass range of 50-550  
114 Da was performed for the detection of the degradation products. MS<sup>n</sup> experiments for  
115 structural elucidation were carried out using 30 % (arbitrary units) collision energy level

116 (CEL). MS data were treated with Analyst® software version 1.5.2 and MS Manager®  
117 software version 12 (ACD Labs, Toronto, Canada). In HR-MS, the ionization conditions were  
118 set as follows: the source voltage was set at 3.4 kV and the temperatures were fixed at 53 °C  
119 (source) and 300 °C (capillary). S-Lens was set at 60%. Acquisition in full scan mode over  
120 the mass range of 300-550 Da was performed for the determination of the degradation  
121 products accurate masses. Data were treated with Xcalibur® software (version 2.2 SP 1.48).  
122 A Q-SUN XE-1 Xenon test chamber (LX 5080 Q-Lab Westlake, California, USA) was used  
123 for photo-degradation studies.

124

## 125 Stress-testing protocol

126

127 The forced degradation solutions were prepared by diluting apixaban stock standard solution  
128 in water or with reagent solutions as to obtain a final concentration of 125 µg mL<sup>-1</sup> of  
129 apixaban in each of them (working solutions). Four stress conditions were tested: thermal,  
130 hydrolytic, photolytic and oxidative conditions. Each experiment was performed in triplicate  
131 and the working solutions were allocated in 5 mL hermetically sealed glass vials. Thermal  
132 stress was achieved at 80 °C up to 7 days. Hydrolysis was studied at room temperature over  
133 a period of 72 hours, using HCl 0.1 M or NaOH 0.1 M. Oxidation was tested in the presence  
134 of an equivalent of 3 % (v/v) H<sub>2</sub>O<sub>2</sub>, at room temperature for 72 h. Photo-degradation  
135 consisted in exposing working solutions to light for 36 h using a xenon test chamber (Q-SUN  
136 Xe-1). Emitted wavelengths ranged from 300 to 800 nm. The light intensity was delivered at  
137 1.50 W/m<sup>2</sup>.

138

## 139 Validation protocol

140

141 An RP-HPLC-UV with stability indicating capability was implemented and validated according  
142 to ICH Q2 (R1)<sup>18</sup>. Specificity was established based on good chromatographic separation

143 and UV detection at 220 nm. The system suitability tests were conducted throughout the  
144 validation studies by injecting  $125 \mu\text{g mL}^{-1}$  of apixaban solution. Peak tailing as well as peak  
145 efficacy was systematically assessed. Linearity and accuracy were studied across  
146 concentration range 25 -  $150 \mu\text{g mL}^{-1}$  of apixaban, through three series of samples  
147 independently prepared. Intermediate precision and repeatability were tested by injection of  
148 six individual solutions of 75 and of  $125 \mu\text{g mL}^{-1}$  apixaban on three consecutive days. Limits  
149 of quantitation (LOQ) and detection (LOD) were determined considering the level of dilution  
150 leading to signal to noise ratios of 10:1 and 3:1, respectively.

151

## 152 RESULTS AND DISCUSSION

153

### 154 Optimised chromatographic conditions and method validation

155

156 Implementing a stability indicating method (SIAM) relies on its capacity to separate apixaban  
157 from its degradation products. After several optimization steps, the method described above  
158 was found suitable for the separation of apixaban from most of the other analytes, in gradient  
159 mode, using water/acetonitrile mobile phase (Table 2, Fig. 1). In such conditions, apixaban  
160 eluted at 13.3 min. The peak-tailing factor ( $A_s$ ) for apixaban was systematically inferior to 1.2  
161 (average of six determinations = 1.15) and the theoretical plates ( $N$ ) was at around 4500  
162 (average of six determinations = 4498). A component detection algorithm (CODA) analysis  
163 also allowed examining the main peak purity, showing that it uniquely contained signals from  
164 apixaban regardless of the sample. Three of the degradation products eluted ahead of the  
165 drug and the rest came after. But the resolution factor ( $R_s$ ) between apixaban and one of the  
166 degradation products (DP-4) was below 1.5 (average of six determinations = 1.32). Mass  
167 balance (% assay + % total degradation products) of all the stressed samples of apixaban  
168 was obtained in the range of 98.2-99.5 %. The regression analysis using a linear model



169 expressing apixaban concentrations as a function of UV chromatogram signals within a  
170 range 25 - 150  $\mu\text{g}\cdot\text{mL}^{-1}$ , resulted in a determination coefficient  $R^2$  of 0.9978 and a y-intercept  
171 of the linear equation which was statistically insignificant ( $p=0.205$ ). The distribution of the  
172 residuals can well be approximated with a normal distribution according to the p-value of the  
173 Shapiro-Wilk normality test ( $p=0.198$ ), so that it could be safely assumed that the calibration  
174 data fitted to a linear model. The LOD and LOQ were of 0.4 and 1.3  $\mu\text{g mL}^{-1}$ , respectively.  
175 The repeatability verified by a six-fold analysis of the concentration level 75  $\mu\text{g mL}^{-1}$  yielded a  
176 RSD inferior to 1.50 %, and the intermediate precision studied over three different days  
177 following the same protocol, led to a RSD equal to 2.09 %.

178 As a result, the method could be used for the assay determination with implementation of  
179 system suitability testing criteria, i.e.  $R_s$  (apixaban/DP-4,  $\geq 1.3$ ),  $A_s$  ( $\leq 1.2$ ) and  $N$  ( $\approx 4500$ ).  
180 Same chromatographic conditions were applied for the characterization of the degradation  
181 products by LC-ESI-HR-MS<sup>n</sup> (Table 1).

182

## 183 Degradation behaviour of apixaban

184

185 Under oxidation, thermal and photolytic stress conditions, neither loss of apixaban nor  
186 appearance of degradation products was detected, which was consistent with what has been  
187 reported recently<sup>12</sup>. Conversely, apixaban was very prone to degradation under hydrolytic  
188 stress. As shown in Table 2, loss of 15 % of apixaban was observed after 24 hours in acidic  
189 conditions, while 11 % was highlighted only after 3 hours in basic conditions.

190 In total, seven degradation products were detected in the solutions subjected to hydrolysis,  
191 when taken at a degradation rate still inferior to 15 %. Even if degradation continued beyond  
192 15 %, we have limited the present study to that of the degradation products formed  
193 precociously in the stress conditions, insofar as the others, sometimes secondarily formed,  
194 can be considered as less likely with respect to real-storage conditions<sup>19</sup>. The studied  
195 degradation products are named "DPn", where n accounts for the elution order. Base

196 hydrolysis resulted DP-1 and DP-2 with relative retention times of 0.65 and 0.73, whereas  
197 acidic degradation chromatograms showed DP-2, DP-3, DP-4, DP-5, DP-6 and DP-7 with  
198 relative retention times of 0.73, 0.96, 1.01, 1.07, 1.16 and 1.21 (Fig. 1, Table 2). Aside from  
199 these DPs, the acidic degradation chromatogram also highlighted the presence of two other  
200 but much less intense compounds, eluted about 10.9 min. But unlike the other ones, they  
201 were not detected in mass spectrometry and therefore, cannot be studied or structurally  
202 elucidated.

203

204 **Fig. 1.** Chromatograms of (a) basic stress sample and (b) acidic stress sample.

205

206 **Table 2.** Forced degradation outcome

207

## 208 Characterization of apixaban and DPs

209

### 210 ESI-MS<sup>n</sup> and ESI-HR-MS<sup>n</sup> fragmentation studies of apixaban

211

212 The drug was initially subjected to LC-MS<sup>n</sup> and to HR-MS<sup>n</sup> analyses to establish its complete  
213 fragmentation pattern, which has not been reported so far. Table 3 lists the precursor and  
214 product ions along with errors (ppm) and elemental compositions obtained from HR-Orbitrap-  
215 MS instrument.

216 Under positive ESI-MS conditions, [M+H]<sup>+</sup> and [M+Na]<sup>+</sup> ions were detected at m/z 460 and  
217 482, respectively. Among the nitrogen functions apixaban is composed of, only carboxamide-  
218 amine function exhibits basic properties with a pKa of 13.1. It is therefore more amenable to  
219 protonation than are the others regarding the ionization process. The ESI-HRMS<sup>2</sup> spectrum  
220 of (M+H)<sup>+</sup> ion yielded 2 product ions with m/z of 461 and 443 (Table 3, Fig. 2a). The first ion  
221 would have been formed by hydrolysis affording a carboxylate derivative (C<sub>25</sub>H<sub>25</sub>N<sub>4</sub>O<sub>5</sub><sup>+</sup>), while  
222 the second would be derived from deamination. Acylium derivative C<sub>25</sub>H<sub>23</sub>N<sub>4</sub>O<sub>4</sub><sup>+</sup> was also

223 shown to have been produced from m/z 461 ion by loss of H<sub>2</sub>O when this one was taken as  
224 precursor during MS<sup>3</sup> study (data not shown). Subjected to the MS<sup>3</sup> process, C<sub>25</sub>H<sub>23</sub>N<sub>4</sub>O<sub>4</sub><sup>+</sup>  
225 (m/z 443) gave rise to the formation of four major product ions with m/z of 415, 282, 241 and  
226 199 (Table 3, Fig. 2b). The other product ions were detected at a much lower intensity and  
227 as discussed later, they turn out to have originated from the previous ones (Fig. 3).

228

229 **Table 3.** High-resolution multistage mass spectrometry data of apixaban.

230

231 **Fig. 2.** High-resolution MS<sup>2</sup> spectrum of (a) the protonated ion of apixaban and (b) high-  
232 resolution MS<sup>3</sup> spectrum of the product ion at m/z 443.

233

234 Transition 443→415 may be related to CO departure by heterolytic cleavage of 3C and the  
235 acyl carbon bond. Carbocation C<sub>24</sub>H<sub>23</sub>N<sub>4</sub>O<sub>3</sub><sup>+</sup> was formed. In turn, C<sub>24</sub>H<sub>23</sub>N<sub>4</sub>O<sub>3</sub><sup>+</sup> only generated  
236 one significantly intense MS<sup>4</sup> product ion (C<sub>23</sub>H<sub>23</sub>N<sub>4</sub>O<sub>2</sub><sup>+</sup>) at m/z 387, by loss of CO (Table 3,  
237 Fig. 3a). According to the scheme (Fig. 4), it was proposed that such a neutral loss would  
238 come from the oxo-piperidin moiety through a rearrangements cascade, triggered by  
239 migration of a hydrogen atom from 9C to 3C through 1,4 H-transfer. The conformation of  
240 C<sub>24</sub>H<sub>23</sub>N<sub>4</sub>O<sub>3</sub><sup>+</sup> is such that thereof would be quite stable by resonance.

241

242 **Fig. 3.** High-resolution MS<sup>4</sup> spectra of the product ions at (a) m/z 415, (b) m/z 282, (c) m/z  
243 241 and (d) m/z 199.

244

245 Elimination of 2-(4-methoxyphenylimino)ethenone was proposed to explain the formation of  
246 m/z 282 ion (Fig. 4). The premise here was that another intermediate (2-(4-methoxyphenyl)-  
247 7-oxo-6-(4-(2-oxopiperidin-1-yl)phenyl)-4,5,6,7-tetrahydro-2H-pyrazolo[3,4-c]pyridine-3-  
248 carbonyl ion) was formed through a rearrangement such as transamination, as illustrated in  
249 Fig. 4. From there, hydrogen migration from 8'C to the H-bond acceptor 1'N, through 1,6 H-  
250 transfer, would have led to the pyrazole ring opening by 1'N-2'N bond cleavage, to the

251 formation of a  $\pi$  bond between 2'N and 3'C, and to the switch of the adjacent double bond.  
252 Eventually, the 161 Da moiety would have been released by heterolytic rupture of 4'C-3'C  
253 bond. When taken as precursor for MS<sup>4</sup> study, C<sub>16</sub>H<sub>16</sub>N<sub>3</sub>O<sub>2</sub><sup>+</sup> (m/z 282) yielded the product  
254 ions at m/z 264, 254 and 240 (Table 1, Fig. 3b), likely by dehydration, CO elimination and by  
255 loss of H<sub>2</sub>C=C=O, respectively. Furthermore, as stated in the proposed fragmentation  
256 scheme of apixaban (Fig. 4), the product ion at m/z 227 would have been generated from  
257 m/z 254 ion by expulsion of HCN.

258

259 **Fig. 4.** Proposed fragmentation patterns of the protonated ions of apixaban, DP-2 and DP-6.

260

261 As for the MS<sup>3</sup> product ion detected at m/z 241 (Fig. 2b), it seemed to have been formed by  
262 loss of a 202 Da moiety, which could in all likelihood be attributed to 1-(4-  
263 (methyleamino)phenyl)piperidin-2-one. As shown in Fig. 4, hydrogen atom migration from  
264 8C to the H-bond acceptor 1N through 1,6 H-transfer, accompanied by a switch of 2N-3C  
265 single bond and of the adjacent double bonds, might have led in the first stage, to the  
266 opening of tetrahydropyridine ring. Next, a similar H-transfer process, that took place  
267 between 2''N and electron-deficient 8''C, would have ended up releasing the aforementioned  
268 neutral fragment by heterolytic cleavage of 8''C-9''C bond. Under the MS<sup>4</sup> conditions (Fig.  
269 3c), C<sub>25</sub>H<sub>23</sub>N<sub>4</sub>O<sub>4</sub><sup>+</sup> appeared to lose two CO to afford the product ion at m/z 185 (C<sub>11</sub>H<sub>9</sub>N<sub>2</sub>O<sup>+</sup>).  
270 The last other important fragmentation route of C<sub>25</sub>H<sub>23</sub>N<sub>4</sub>O<sub>4</sub><sup>+</sup> (m/z 443) was represented by  
271 transition 443→199. Thereof would be formed by loss of a 216 Da moiety and of CO. 1-(4-  
272 isocyanatophenyl)piperidin-2-one could possibly account for the so-called 216 Da moiety.  
273 Indeed, it was proposed that by tautomerism, electron-deficient 5C had withdrawn a hydrogen  
274 atom to 9C, leading to the formation of a  $\pi$  bond between 4C and 9C. From there, switch of  
275 C9-C8 and 7N-8C single bonds would have allowed generating a metastable ion with m/z of  
276 227, which in turn, would have undergone CO loss to afford m/z 199 ion (Fig. 4). When taken  
277 as precursor for MS<sup>4</sup> study, m/z 199 ion could notably produce m/z 172 ion by elimination of  
278 HCN (Fig. 3d).

279 Throughout this study, the product ions presented in Fig. 4 were all confirmed by accurate  
280 mass measurement.

281

### 282 **Identification of the degradation products by LC-HR-MS and LC-MS<sup>n</sup>**

283

284 **DP-1** gave a protonated ion with  $m/z$  of 478. Having 18 Da greater than that of apixaban, it  
285 could be considered as a hydrolysis product (Table 4). Indeed, its  $MS^2$  spectrum also  
286 includes  $m/z$  460 ion and some of the major product ions described above, i.e.  $m/z$  227, 199,  
287 184 and 172 ions, suggesting that the protonated ion of DP-1 could lose  $H_2O$  to afford  
288 apixaban  $[M+H]^+$  ion, thus restoring the amide bond. Aside from this fragmentation path, the  
289 mass spectrum also exhibited abundant product ions at  $m/z$  461, 417, 288, 271, 203 and 217  
290 (Table 2, Fig. 5a). The ion at  $m/z$  461 may be due to  $NH_3$  expulsion revealing the presence of  
291 carboxamide function. Transition  $461 \rightarrow 417$  would correspond to  $CO_2$  elimination caused by  
292 the presence of carboxylate function, demonstrating that DP-1 was well been formed by  
293 hydrolysis of an amide bond. In addition, opening of the oxopiperidin ring by hydrolysis of the  
294 amide bond could easily explain the formation of  $m/z$  288 ion by loss of oxopiperidinylaniline  
295 group through N-dealkylation (Fig. 6). Such a characteristic product ion could in turn lose  
296  $NH_3$  to generate  $m/z$  271 ion. The other abundant product ions would have been formed from  
297 the protonation of aniline-amine function as shown in Fig. 6. The ion at  $m/z$  191 would be  
298 produced through N-dealkylation, while  $m/z$  203 ion would be the result of the Mac-Lafferty  
299 rearrangement. As a result, DP-1 could be identified as 3-carbamoyl-1-(4-methoxyphenyl)-4-  
300 (2-(4-(2-oxopiperidin-1-yl)phenylamino)ethyl)-1*H*-pyrazole-5-carboxylic acid. This structure  
301 was also confirmed by the accurate mass measure of DP-1 (Table 4).

302

303 **Table 4.** Retention times, accurate masses with errors, elemental compositions and  $MS^2$   
304 relevant product ions of the degradation products.

305

306 **Fig. 5.**  $MS^2$  spectra of the protonated ions of (a) DP-1, (b) DP-4 and (c) DP-7.

307

308 **Fig. 6.** Proposed fragmentation pattern of the protonated ion of DP-1.

309

310 MS/MS product ions of **DP-2 and DP-6** were almost all the same as that of apixaban. Only  
311 the protonated precursor ions were different (Table 4). Instead of transition 460→443  
312 corresponding to loss of NH<sub>3</sub>, transitions 461→443 and 475→443 took place for DP-2 and  
313 DP-6, respectively. They might correspond to dehydration and loss of methanol (Fig. 4). As a  
314 result, DP-2 and DP-6 might correspond to 1-(4-methoxyphenyl)-7-oxo-6-(4-(2-oxopiperidin-  
315 1-yl)phenyl)-4,5,6,7-tetrahydro-1*H*-pyrazolo[3,4-*c*]pyridine-3-carboxylic acid and to methyl-1-  
316 (4-methoxyphenyl)-7-oxo-6-(4-(2-oxopiperidin-1-yl)phenyl)-4,5,6,7-tetrahydro-1*H*-  
317 pyrazolo[3,4-*c*]pyridine-3-carboxylate, respectively. These structures were also confirmed by  
318 the accurate mass measure of DP-2 and DP-6 (Table 4).

319

320 As DP-1, **DP-4** yielded a protonated ion with *m/z* of 478. Therefore, it could equally be  
321 considered as a hydrolysis product (Table 4). Its MS<sup>2</sup> spectrum includes common ions with  
322 that of apixaban as was already mentioned for DP-1. It also displays extra product ions with  
323 *m/z* of 432, 416, 404, 390, 378, 361, 333, 300 and 101 (Fig. 5b). The presence of some of  
324 them confirmed that the oxo-piperidin ring opening had occurred by hydrolysis of the amide  
325 bond. The ion at *m/z* 101 may be due to N-C bond heterolytic cleavage releasing *n*-pentanoic  
326 acid carbocation. The product ion at *m/z* 378 would have been formed through N-  
327 dealkylation after the protonation of aniline-amine function. The anilinium derivative could in  
328 turn successively lose NH<sub>3</sub> and CO to yield *m/z* 361 and *m/z* 333 ions, respectively. As  
329 shown in Fig. 7, existence of some of the product ions could be related to the C-C bonds  
330 rupture on the lateral chain. This seems to concern the product ions at *m/z* 432, 416 and  
331 404. Aside from the fragmentation paths involving the lateral chain, elimination of 2-(4-  
332 methoxyphenylimino)ethenone that was already described for apixaban, would have  
333 generated *m/z* 300 ion, which in turn, would have lost a water molecule to afford *m/z* 282 ion.  
334 Similarly, loss of an isocyanatophenyl derivative along with CO would have formed *m/z* 199

335 ion. Therefore, such a fragmentation pattern is entirely consistent with the protonated ion of  
336 5-(4-(3-carbamoyl-1-(4-methoxyphenyl)-7-oxo-4,5-dihydro-1*H*-pyrazolo[3,4-*c*]pyridin-6(7*H*)-  
337 yl)phenylamino)pentanoic acid, as precursor.

338

339 **Fig. 7.** Proposed fragmentation patterns of the protonated ions of DP-4 and DP-7.

340

341 **DP-7** protonated ion was detected at *m/z* 492. Its accurate mass, measured by HR-MS, is  
342 consistent with C<sub>30</sub>H<sub>26</sub>N<sub>5</sub>O<sub>5</sub><sup>+</sup> elemental formula (Table 4, Fig. 5c). Given a perfect parallelism  
343 between the fragmentation patterns of DP-4 and **DP-7** (Table 2, Fig. 5 and 7), DP-7 was  
344 identified as methyl 5-(4-(3-carbamoyl-1-(4-methoxyphenyl)-7-oxo-4,5-dihydro-1*H*-  
345 pyrazolo[3,4-*c*]pyridin-6(7*H*)-yl)phenylamino)pentanoate.

346

347 **DP-3 and DP-5** were also found to include the characteristic fragments *m/z* 361 and *m/z* 333  
348 within their ESI-MS/MS spectra. Moreover, by comparing the elemental formula of  
349 protonated DP-3 and of DP-5 to that of the drug (Table 4), it was easy to demonstrate that  
350 they corresponded to aniline derivatives having lost the oxo-piperidin group. In addition, it  
351 seems that DP-3 would carry a carboxylate group and DP-5 a carboxymethyl group instead  
352 of the initial carboxamide function (Table 4). These assumptions were further supported by  
353 the determination of their fragmentation pattern such described by Fig. 8. Loss of water and  
354 of methanol from protonated DP-3 and DP-5, respectively, was observed through the  
355 presence of *m/z* 361 ion on both MS<sup>2</sup> spectra. The protonated ion of DP-3 also corresponds  
356 to a product ion of the protonated ion of DP-5 after demethylation. As the degradation  
357 products structure had preserved the tetrahydropyridine-pyrazolo-methoxyphenyl core, it was  
358 logical that the transition involving loss of 2-(4-methoxyphenylimino)ethenone (361 → 200)  
359 was one more time detected. Always from the product ion at *m/z* 361, *m/z* 241 and *m/z* 199  
360 ions would have been produced according to the same mechanisms as those described for  
361 apixaban, as shown in Fig. 8. As a result, DP-3 might correspond to 6-(4-aminophenyl)-1-(4-  
362 methoxyphenyl)-7-oxo-4,5,6,7-tetrahydro-1*H*-pyrazolo[3,4-*c*]pyridine-3-carboxylic acid and

363 DP-5, to methyl-6-(4-aminophenyl)-1-(4-methoxyphenyl)-7-oxo-4,5,6,7-tetrahydro-1*H*-  
364 pyrazolo[3,4-*c*]pyridine-3-carboxylate.

365

366 **Fig. 8.** MS<sup>2</sup> mass spectrum of the protonated ions of DP-3 (a) and DP-5 (b) and their  
367 corresponding fragmentation patterns. Some common remarkable transitions are featured on  
368 the MS/MS spectrum of DP-5 (b).

369

370 **Proposed degradation pathways of apixaban.**

371

372 Given the outcome from the stress studies, it was clear that apixaban was more susceptible  
373 to acidic and alkali conditions than to the other tested conditions. It seems that the oxo-  
374 piperidin group was more amenable to acidic hydrolysis and that the oxo-tetrahydropyridine  
375 was more sensible to alkali conditions, according to the study conditions. Hydrolysis of the  
376 caboxamide function seemed to occur under one or the other condition. The carboxymethyl  
377 derivatives would have been formed in the presence of methanol, used for dissolution of  
378 apixaban API prior to being subjected to stress conditions. But under the alkali conditions,  
379 esterification should not occur or if it were the case, then the esters formed would have been  
380 saponified. The schematic representations of mechanism of formation of the degradation  
381 products under hydrolytic stress are depicted in Fig. 9.

382

383 **Fig. 9.** Proposed degradation patterns of apixaban under stress conditions.

384

## 385 Conclusion

386 The degradation behaviour of apixaban under hydrolytic (acid, base), oxidative, photolytic  
387 and thermal stress conditions was studied as per ICH guidelines. Degradation studies  
388 demonstrated that apixaban was more fragile with respect to hydrolysis conditions. Its MS<sup>n</sup>



389 fragmentation scheme was studied in depth in order to help assign, by comparison, the  
390 structures of the product ions formed from the degradation products. A total of seven  
391 degradation products were highlighted in the samples exposed to hydrolysis conditions,  
392 having reached a degradation rate at maximum of 15 %. Based on their identification, it was  
393 possible to deduct major degradation mechanisms in the context of stress testing.  
394 A stability-indicating LC method was developed and it has shown suitable for the drug  
395 quantification as well as for the impurity determination.

396

## 397 References

- 398 1 P.C. Wong, E.J. Crain, B. Xin, R.R. Wexler, P.Y. Lam, D.J. Pinto, J.M. Luetzgen, R.M.  
399 Knabb, *J. Thromb. Haemost.*, 2008, **6**, 820-9.
- 400 2 P.C. Wong, C.A. Watson, E.J. Crain, *J. Thromb. Haemost.*, 2008, **6**, 1736-41.
- 401 3 P.C. Wong, E.J. Crain, C.A. Watson, B. Xin, *J. Thromb. Haemost.*, 2009, **7**, 1313-20.
- 402 4 B.I. Eriksson, D.J. Quinlan, J.I. Weitz, *Clin. Pharmacokinet.*, 2009, **48**, 1-22.
- 403 5 M.R. Lassen, G.E. Raskob, A. Gallus, G. Pineo, D. Chen, P. Hornick, *Lancet*, 2010, **375**,  
404 807-15.
- 405 6 M.R. Lassen, A. Gallus, G.E. Raskob, G. Pineo, D. Chen, L.M. Ramirez, *N. Engl. J. Med.*,  
406 2010, **363**, 2487-98.
- 407 7 K. He, J.M. Luetzgen, D. Zhang, B. He, J.E. Grace Jr., B. Xin, D.J.P. Pinto, P.C. Wong, R.M.  
408 Knabb, P.Y.S. Lam, R.R. Wexler, S.J. Grossman, *Eur. J. Drug Metab. Pharmacokinet.*, 2011,  
409 **36**, 129-139.
- 410 8 E.M. Schmitz, K. Boonen, D.J. van den Heuvel, J.L. van Dongen, M.W. Schellings, J.M.  
411 Emmen, F. van der Graaf, L. Brunsveld, D. van de Kerkhof, *J. Thromb. Haemost.*, 2014,  
412 **12**(10),1636-46.
- 413 9 D. Zhang, K. He, N. Raghavan, L. Wang, E.J. Crain, B. He, B. Xin, J.M. Luetzge, P.C. Wong,  
414 *J. Thromb. Thrombolysis*, 2010, **29**, 70-80.
- 415 10 X. Delavenne, P. Mismetti, T. Basset, *J. Pharm. Biomed. Anal.*, 2013, **78-79**, 150-153.

- 416 11 P.C. Wong, D. Zhang, *Drug Metab. Dispos.*, 2009, **37**, 74-81.
- 417 12 S.S. Prabhune, R.S. Jaguste, P.L. Kondalkar, N.S. Pradhan, *Sci. Pharm.*, 2014, **82**, 777–  
418 785.
- 419 13 P. Lebel, J. Gagnon, A. Furtos, K.C. Waldron, *J. Chromatogr. A*, 2014, **1343**, 143-151.
- 420 14 S. Singh, T. Handa, M. Narayanam, A. Sahu, M. Junwal and S. Gorog, *Trends Anal. Chem.*,  
421 2006, **25**, 755-757.
- 422 15 R.P. Shah, *J. Pharm. Biomed. Anal.*, 2012, **69**, 148-173.
- 423 16 R. N. Rao and A.N. Raju, *J. Sep. Sci.*, 2006, **29**, 2733-2744.
- 424 17 R. N. Rao, K. Ramakrishna, B. Sravan and K. Santhakumar, *J. Pharm. Biomed. Anal.*, 2013,  
425 **77**, 49-54.
- 426 18 ICH Guideline Q2 (R1), Validation of Analytical Procedures, Text and Methodology,  
427 November 2005.
- 428 19 Blessy M., Ruchi D. Patel, Prajesh N. Prajapati, Y.K. Agrawal, *J. Pharm. Anal.*, 2014,  
429 **4**, 159–165.
- 430
- 431
- 432
- 433
- 434
- 435
- 436
- 437
- 438
- 439
- 440
- 441
- 442

## 443 Tables

444

445 **Table 1.** HPLC gradient

Time (min)	A : Water (% v/v)	B : Acetonitrile (% v/v)
0→2	95	5
2→13	95→40	5→60
13→19	40	60
19→20	40→95	60→5

446

447 **Table 2.** Forced degradation outcome (n=3)

448

<b>Stress condition</b>	<b>Time</b>	<b>Average assay of API (% w/w, n=3)</b>	<b>Average total impurities (% w/w, n=3)</b>	<b>Average mass balance (assay + total impurities %, n=3)</b>	<b>Commentaries</b>
<b>Acid hydrolysis (0.1 M HCl)</b>	24 hours	84.9	14.6	99.5	Degradation accompanied by appearance of DP-2, DP-3, DP-4, DP-5, DP-6 and DP-7
<b>Base hydrolysis (0.1 M NaOH)</b>	3 hours	88.1	10.8	98.9	Degradation accompanied by appearance of DP-1 and DP-2
<b>Oxidation (3 % H<sub>2</sub>O<sub>2</sub>)</b>	72 hours	99.3	N.D.	99.3	No degradation occurred
<b>Thermal (80°C)</b>	7 days	99.5	N.D.	99.5	No degradation occurred
<b>Photolysis (UV light)</b>	36 hours	98.6	N.D.	98.6	No degradation occurred

449

450

451

452

453

454

455 **Table 3.** MS<sup>n</sup> and high-resolution MS<sup>n</sup> data of apixaban.

Product ions m/z	Origin	Best possible elemental formula	Theoretical masses m/z	Accurate masses m/z	Error (ppm)
460	[M+H] <sup>+</sup>	C <sub>25</sub> H <sub>26</sub> N <sub>5</sub> O <sub>4</sub> <sup>+</sup>	460.19793	460.19655	-3.00 <sup>458</sup>
461	MS <sup>2</sup> (460→)	C <sub>25</sub> H <sub>25</sub> N <sub>4</sub> O <sub>5</sub> <sup>+</sup>	461.18195	461.18054	-3.06 <sup>459</sup>
443	MS <sup>2</sup> (460→)	C <sub>25</sub> H <sub>23</sub> N <sub>4</sub> O <sub>4</sub> <sup>+</sup>	443,171382	443,17006	-2,98
415	MS <sup>3</sup> (460→443→)	C <sub>24</sub> H <sub>23</sub> N <sub>4</sub> O <sub>3</sub> <sup>+</sup>	415,176467	415,17547	-2,40 <sup>460</sup>
387	MS <sup>4</sup> (460→443→415→)	C <sub>23</sub> H <sub>23</sub> N <sub>4</sub> O <sub>2</sub> <sup>+</sup>	387,18155	387,18073	-2,12
282	MS <sup>3</sup> (460→443→)	C <sub>16</sub> H <sub>16</sub> N <sub>3</sub> O <sub>2</sub> <sup>+</sup>	282,123703	282,12279	-3,24 <sup>461</sup>
264	MS <sup>4</sup> (460→443→282→)	C <sub>16</sub> H <sub>14</sub> N <sub>3</sub> O <sup>+</sup>	264,11370	264,1122	-5,68
254	MS <sup>4</sup> (460→443→282→)	C <sub>15</sub> H <sub>16</sub> N <sub>3</sub> O <sup>+</sup>	254,128789	254,12791	-3,46 <sup>462</sup>
241	MS <sup>3</sup> (460→443→)	C <sub>13</sub> H <sub>9</sub> N <sub>2</sub> O <sub>3</sub> <sup>+</sup>	241,06077	241,06004	-3,03 <sup>463</sup>
240	MS <sup>4</sup> (460→443→282→)	C <sub>14</sub> H <sub>14</sub> N <sub>3</sub> O <sup>+</sup>	240,11314	240,11228	-3,58
227	MS <sup>4</sup> (460→443→282→)	C <sub>14</sub> H <sub>15</sub> N <sub>2</sub> O <sup>+</sup>	227,11789	227,11711	-3,43 <sup>464</sup>
199	MS <sup>3</sup> (460→443→)	C <sub>12</sub> H <sub>11</sub> N <sub>2</sub> O <sup>+</sup>	199,086589	199,08620	-1,95
185	MS <sup>4</sup> (460→443→241→)	C <sub>11</sub> H <sub>9</sub> N <sub>2</sub> O <sup>+</sup>	185,070939	185,07035	-3,18 <sup>465</sup>
172	MS <sup>4</sup> (460→443→199→)	C <sub>11</sub> H <sub>10</sub> NO <sup>+</sup>	172,07569	172,07516	-3,08 <sup>466</sup>

467

468

469

470

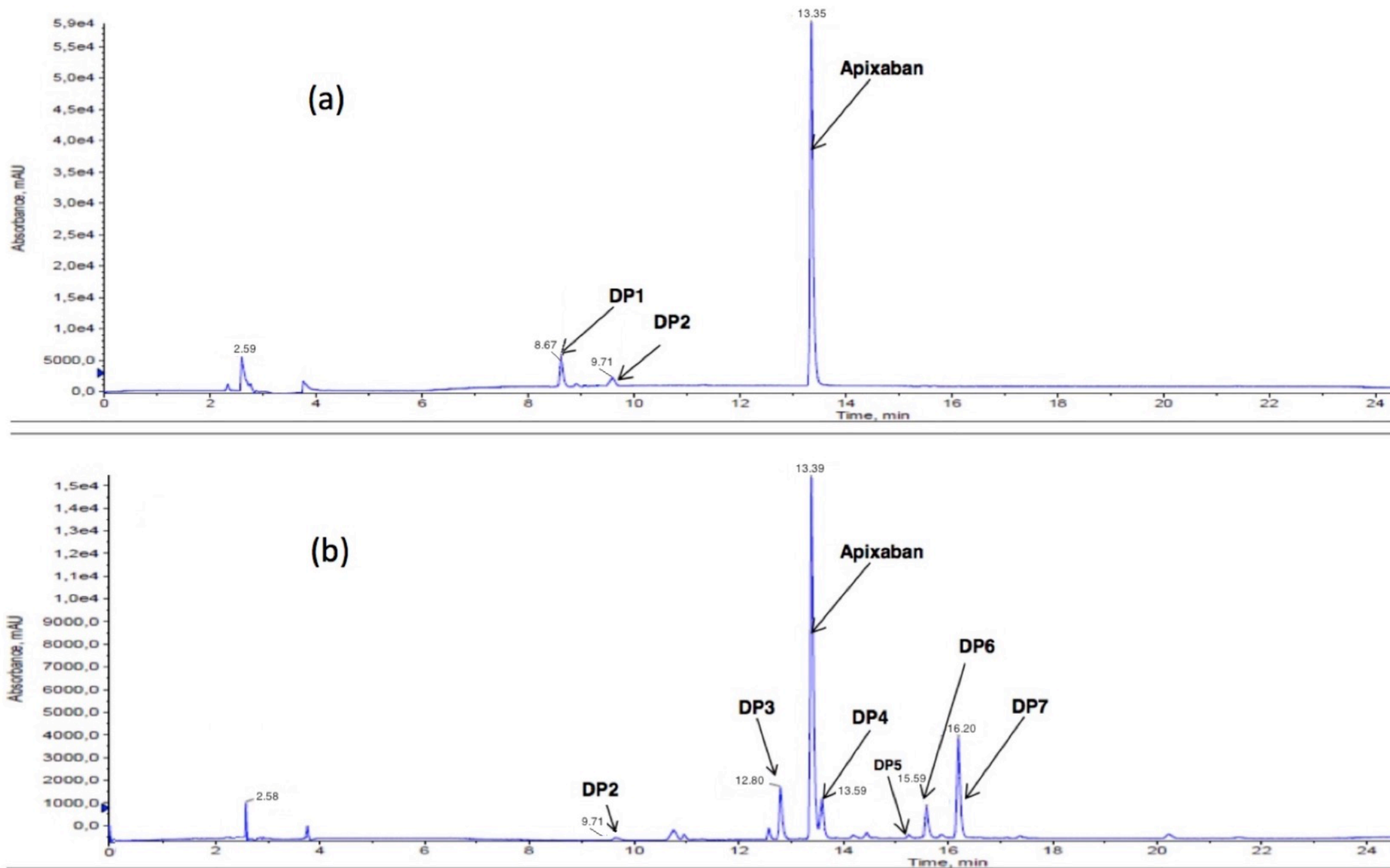
471

472

473 **Table 4.** Retention times, accurate masses with errors, elemental compositions and MS<sup>2</sup> relevant product ions of the degradation product

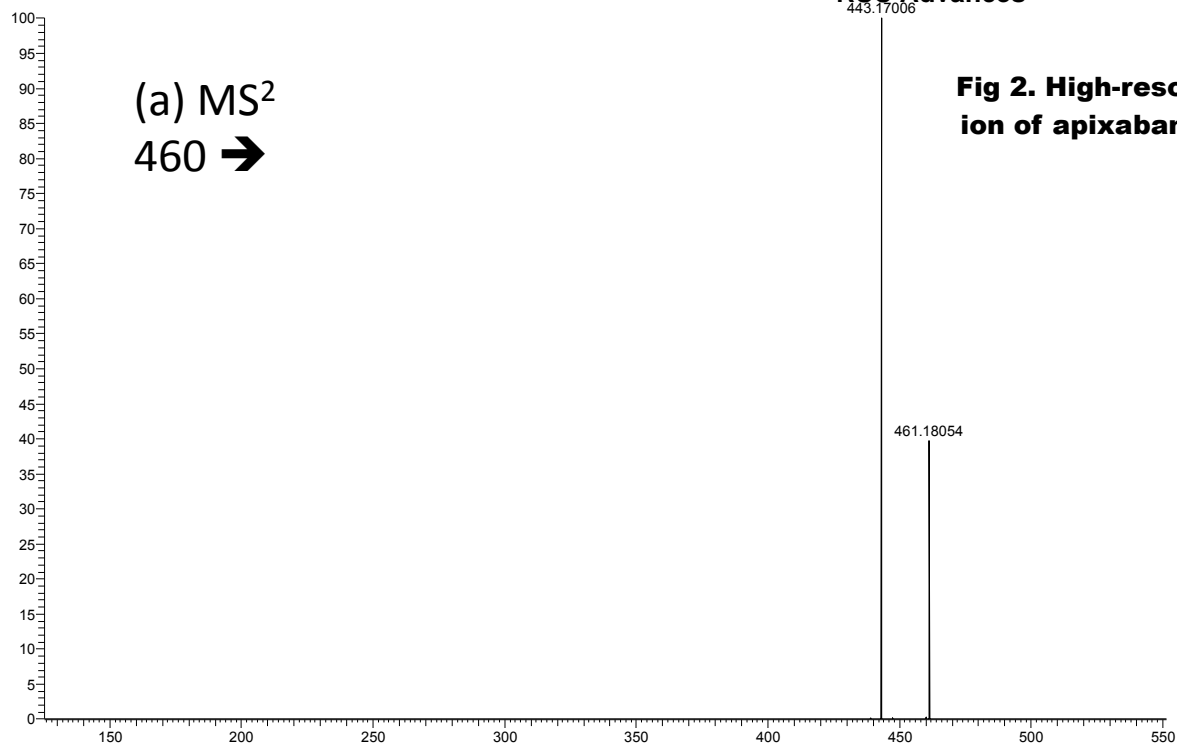
Products	rT (min)	Conditions	[M+H] <sup>+</sup>	Elemental compositions	Theoretical masses	Accurate masses with error in ppm	Relevant MS/MS product ions assigned (m/z)
<b>DP-1</b>	8,7	Basic	478	C <sub>25</sub> H <sub>28</sub> N <sub>5</sub> O <sub>5</sub> <sup>+</sup>	478.20849	478.20755 (-1.97)	461 ; 460 ; 417 ; 288 ; 271 ; 244 ; 227 ; 203 ; 199 ; 191
<b>DP-2</b>	9,7	Acidic/Basic	461	C <sub>25</sub> H <sub>25</sub> N <sub>4</sub> O <sub>5</sub> <sup>+</sup>	461.18195	461.18090 (-2.28)	443 ; 415 ; 387 ; 282 ; 254 ; 227 ; 199 ; 185 ; 172
<b>DP-3</b>	12,8	Acidic	379	C <sub>20</sub> H <sub>18</sub> N <sub>4</sub> O <sub>4</sub> <sup>+</sup>	379.14008	379.13883 (-3.30)	361 ; 333 ; 303 ; 241 ; 200 ; 199 ; 185 ; 172
<b>Apixaban</b>	13,3	–	460	C <sub>25</sub> H <sub>26</sub> N <sub>5</sub> O <sub>4</sub> <sup>+</sup>	460.19793	460.19674 (-2.59)	See Table 1
<b>DP-4</b>	13,6	Acidic	478	C <sub>25</sub> H <sub>28</sub> N <sub>5</sub> O <sub>5</sub> <sup>+</sup>	478.20849	478.20702 (-3.07)	461 ; 460 ; 443 ; 432 ; 416 ; 404 ; 390 ; 378 ; 361 ; 333 ; 300 ; 282 ; 199 ; 185 ; 101
<b>DP-5</b>	14,6	Acidic	393	C <sub>21</sub> H <sub>21</sub> N <sub>4</sub> O <sub>4</sub> <sup>+</sup>	393.15573	393.15436 (-3.48)	393 ; 379 ; 361 ; 333 ; 241 ; 200 ; 199 ; 185 ; 172 ; 156
<b>DP-6</b>	15,6	Acidic	475	C <sub>26</sub> H <sub>27</sub> N <sub>4</sub> O <sub>5</sub> <sup>+</sup>	475.19760	475.19621 (-2.93)	475 ; 461 ; 443 ; 282 ; 254 ; 241 ; 227 ; 199 ; 185 ; 172 ; 156
<b>DP-7</b>	16,2	Acidic	492	C <sub>26</sub> H <sub>30</sub> N <sub>5</sub> O <sub>5</sub> <sup>+</sup>	492.22415	492.22257 (-3.21)	475 ; 432 ; 416 ; 404 ; 390 ; 378 ; 377 ; 371 ; 333 ; 314 ; 282 ; 227 ; 199 ; 185 ; 115

474

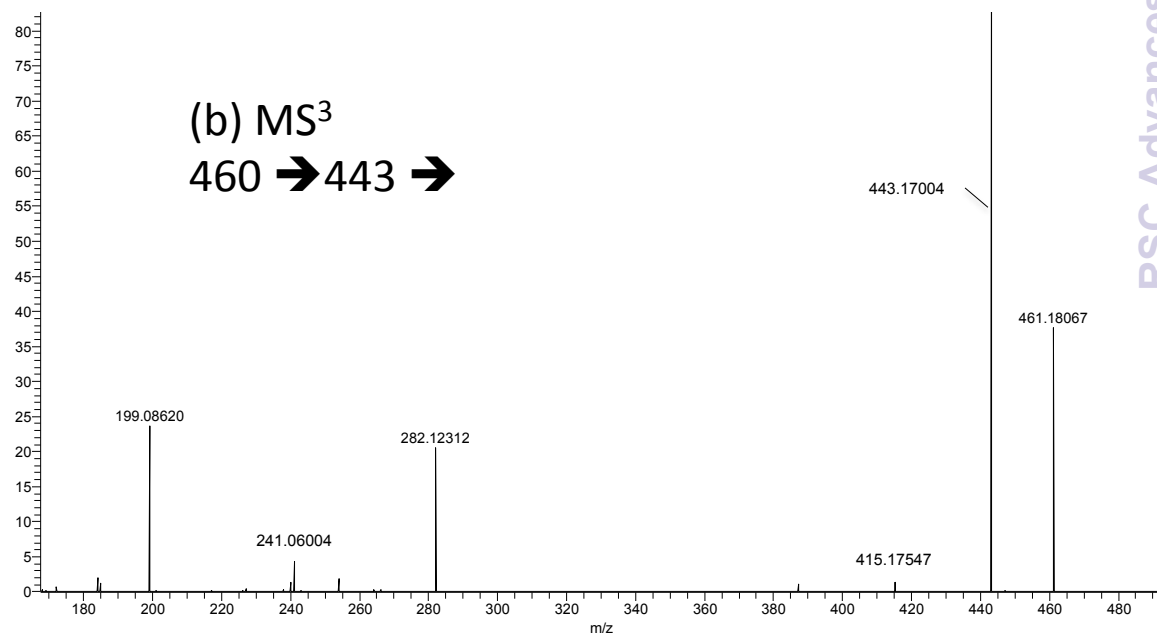


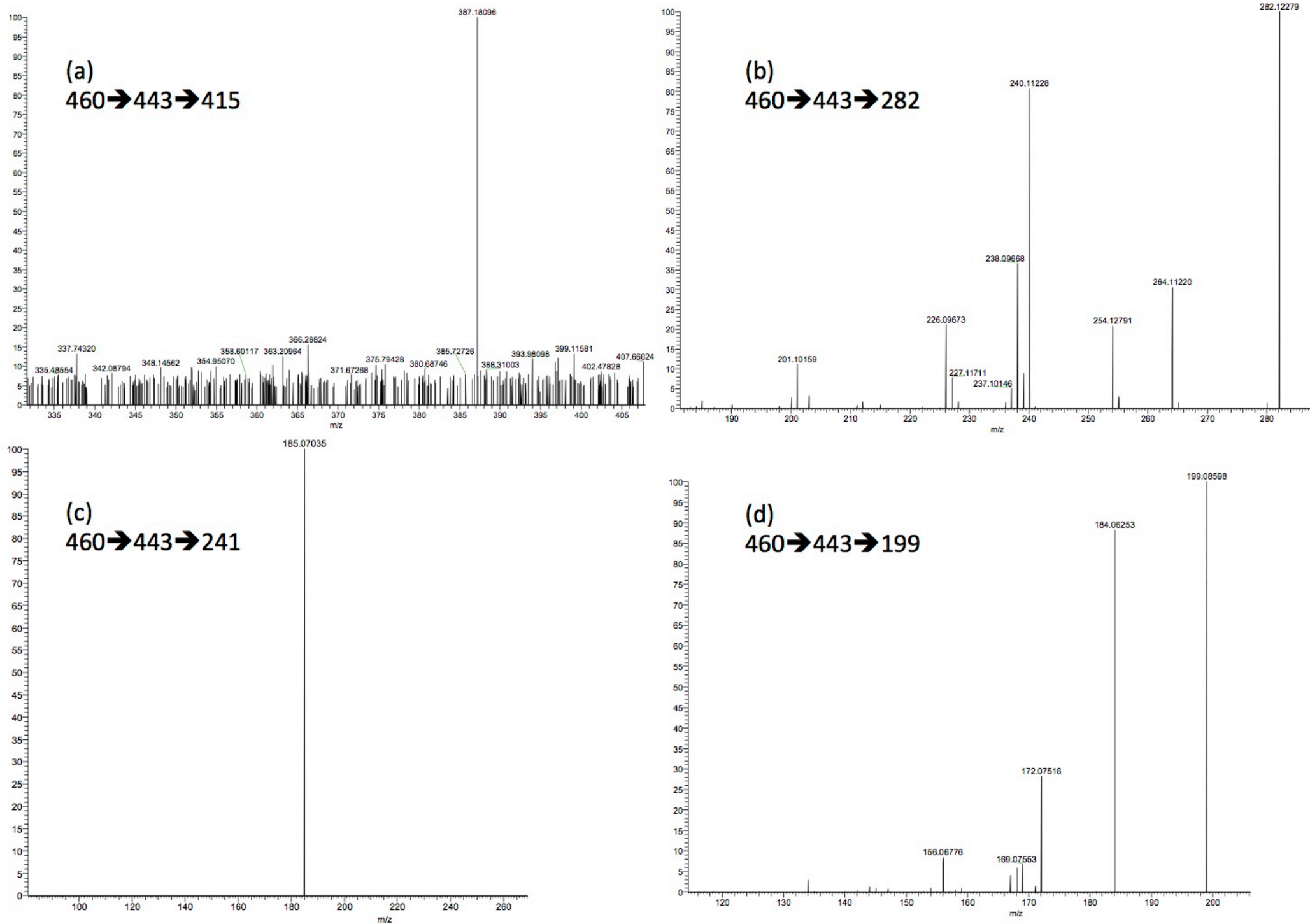
**Fig 1. Chromatograms of (a) basic stress sample and (b) acidic stress sample**



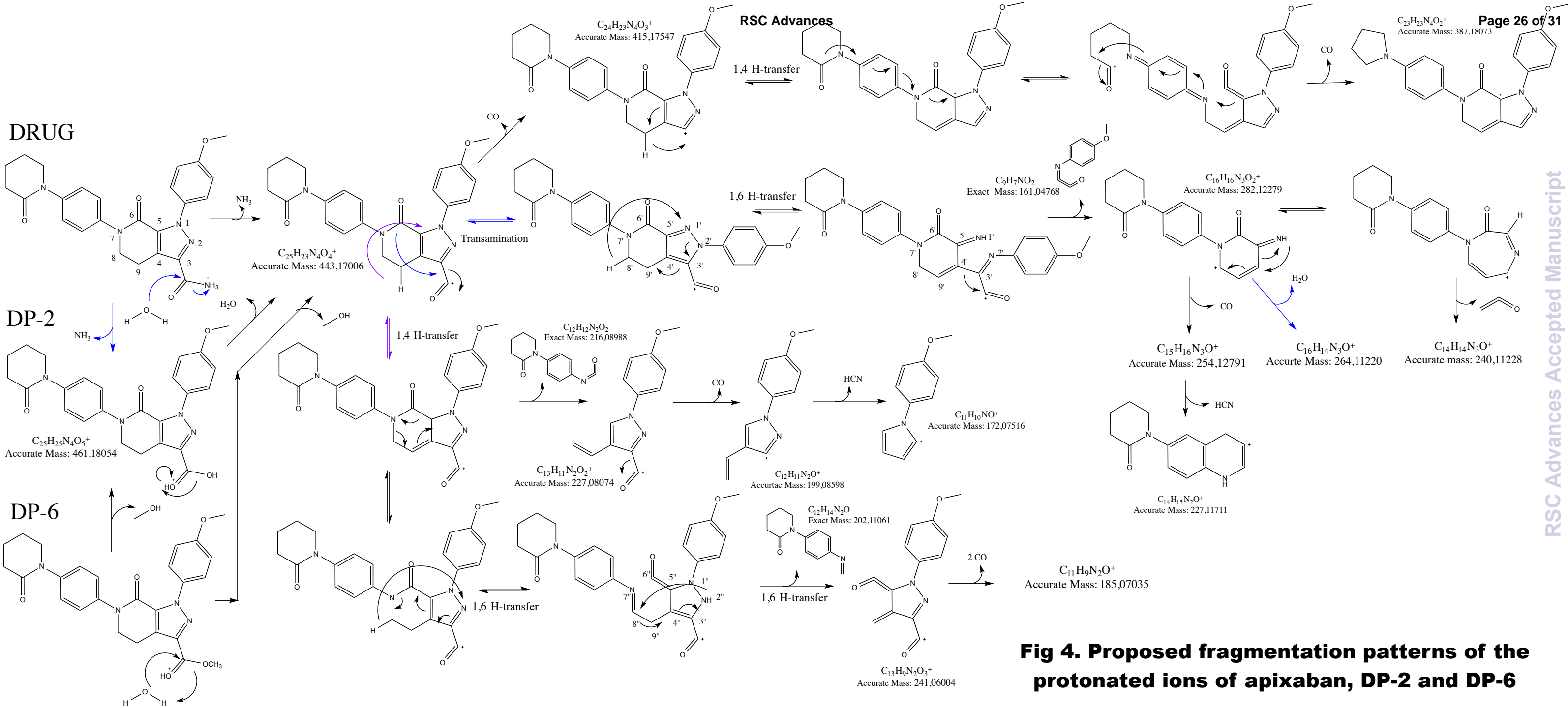


**Fig 2. High-resolution MS/MS spectrum of (a) the protonated ion of apixaban and (b) high-resolution MS/MS/MS spectrum of the product ion at m/z 443**





**Fig 3 High-resolution MS4 spectra of the product ions at (a) m/z 415, (b) m/z 282, (c) m/z 241 and (d) m/z 199**



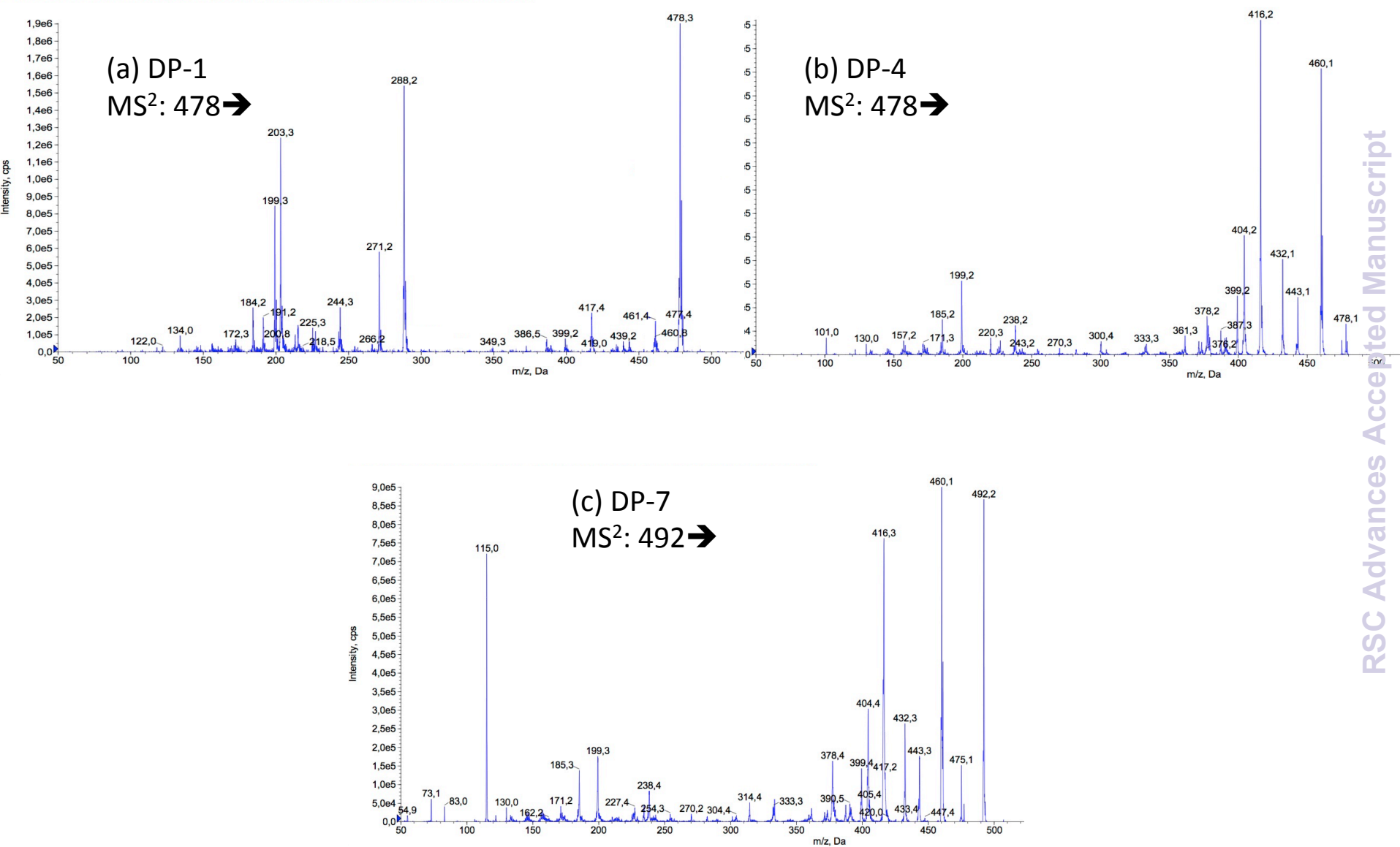


**Fig 5. MS/MS spectra of the protonated ions of (a) DP-1, (b) DP-4 and (c) DP-7**



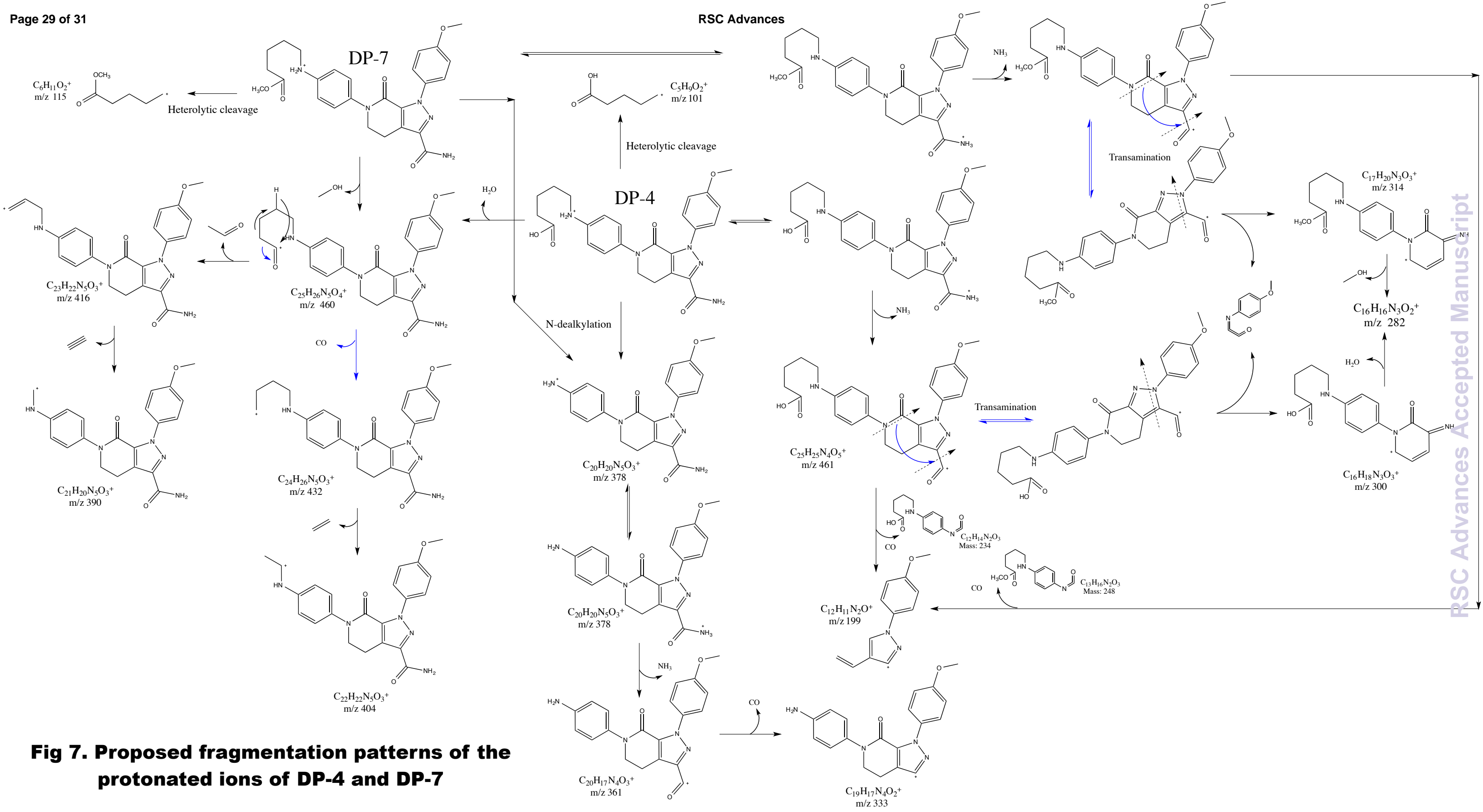
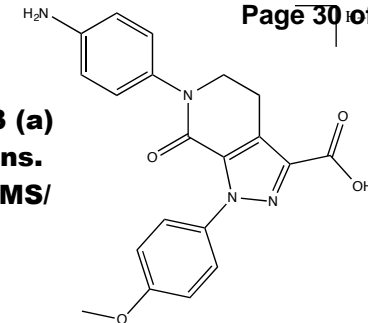
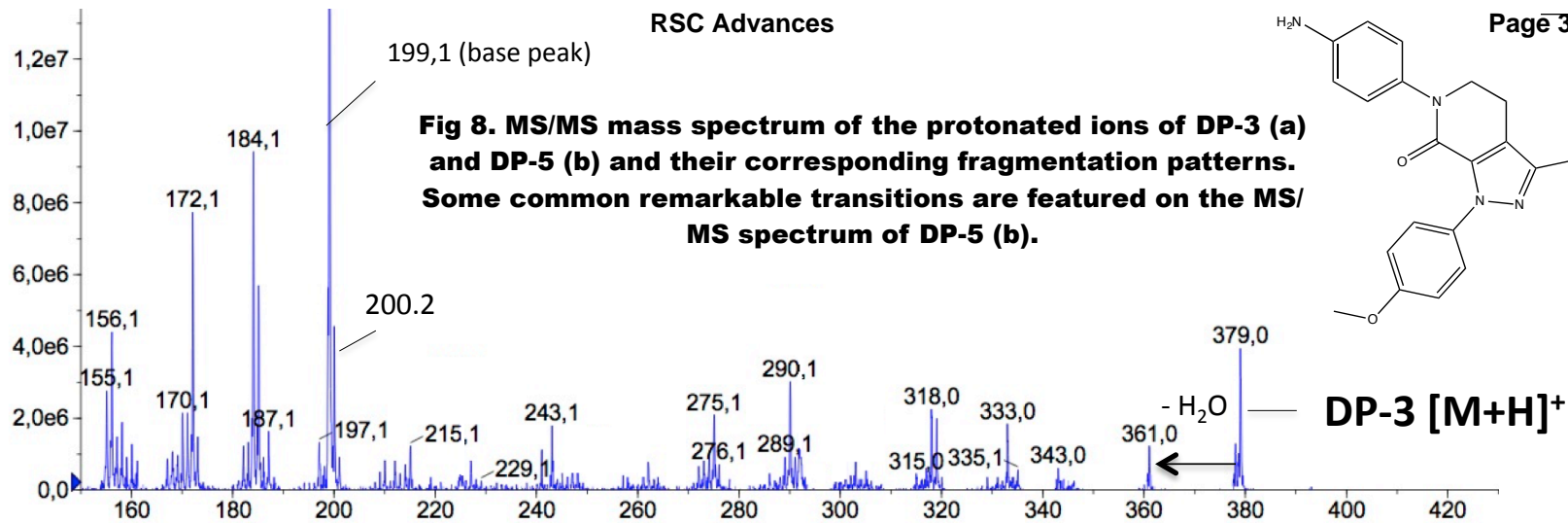


**Fig 7. Proposed fragmentation patterns of the protonated ions of DP-4 and DP-7**

(a)



(b)

